HTRA1-TARGETED SMALL MOLECULES AS THERAPIES FOR ALZHEIMER'S DISEASE

William Lin [1]

[1] Saint Francis High School

Abstract

Alzheimer's disease remains one of the most pressing neurodegenerative disorders, with limited treatment options, making the identification of novel therapeutic targets a crucial research challenge. In this study, we focused on the HtrA serine peptidase 1 (HTRA1) receptor, which plays a key role in disease pathology. First, we applied three complementary binding-site prediction tools – DogSiteScorer (DOG algorithm), FTSite (FFT solvent mapping), and Prank-Web (PRANK deep learning)—to the HTRA1 crystal structure, identifying five high-confidence pockets. Next, a pharmacophore model was built in Pharmit to capture key hydrogen bond donors/acceptors and hydrophobic/aromatic features; screening of a ~150,000-compound library yielded 15 diverse candidates. These 15 ligands were docked using SwissDock and ranked by estimated binding free energy (ΔG) and full-fitness scores. The top five compounds ($\Delta G \leq -7.5$ kcal/mol, exhibiting consistent hydrogen bonds with active-site residues) advanced to ADME and toxicity evaluation. ADME properties were predicted via SwissADME, enforcing Lipinski's Rule of Five and Veber's rules (TPSA ≤ 140 Å²; ≤ 10 rotatable bonds), while toxicity risks were assessed using ProTox-3 (hepatotoxicity, carcinogenicity, LD_{50}). Finally, molecular dynamics simulations (100-ns GROMACS runs) on the best three candidates (GlideScores < -8.5 kcal/mol; RMSD < 2 Å; $\geq 80\%$ key H-bond occupancy) confirmed stable binding. These three lead molecules, selected for their optimal binding affinity, dynamic stability, and favorable ADME/toxicity profiles, now proceed to in vitro validation – paving the way toward a targeted Alzheimer's therapy with high efficacy and minimal side effects.

Keywords: *Alzheimer's disease, drug discovery, small molecules, HTRA1, pharmacophore, virtual screening*

1. Introduction

Alzheimer's disease (AD) is a progressive neurodegenerative disorder and the most common cause of dementia. It is characterized by cognitive decline, memory loss, and behavioral changes, ultimately leading to a complete loss of independence (Scheltens et al., 2021).

Despite extensive research, the exact mechanisms underlying Alzheimer's disease (AD) remain complex and multifaceted, involving genetic, molecular, and environmental factors (Heneka et al., 2015; Heppner et al., 2015).

Three significant hypotheses explain Alzheimer's disease (AD) pathogenesis: the

amyloid hypothesis, the cholinesterase hypothesis, and the neuroinflammation hypothesis. The amyloid hypothesis posits that the accumulation of amyloid-beta (Aβ) triggers a cascade of neurotoxic events, including tau protein dysfunction and neuronal death (Kurkinen et al., 2023; Hardy & Higgins, 1992; Selkoe & Hardy, 2016). The cholinesterase hypothesis posits that cognitive decline arises from the degeneration of cholinergic neurons and the ensuing deficiency in acetylcholine (Orhan, 2021; Bartus et al., 1982; Hampel et al., 2018). Meanwhile, the neuroinflammation hypothesis highlights the role of chronic brain inflammation in exacerbating neuronal damage and accelerating disease progression (Lecca et al., 2022; Heneka et al., 2015; Heppner et al., 2015).

Currently, medications such as cholinesterase inhibitors (donepezil, rivastigmine, galantamine) and memantine help manage Alzheimer's disease (AD) symptoms by improving neurotransmitter function (Alzheimer's Association, n.d.; Hampel et al., 2018). Recently, monoclonal antibodies such as aducanumab and lecanemab have been approved for targeting amyloid-beta plaques, although their efficacy remains controversial (Cummings et al., 2021; Knopman et al., 2021). These treatments offer limited success, focusing mainly on symptom management rather than halting disease progression, highlighting the need for new therapies targeting the underlying mechanisms of AD.

Recent research has identified high-temperature requirement serine protease A1 (HTRA1) as a potential player in Alzheimer's disease (AD) pathology. HTRA1 is a serine protease involved in protein degradation and cellular homeostasis, and emerging evidence suggests its dysregulation is linked to neurodegenerative diseases (Chen et al., 2024; Zurawa-Janicka et al., 2010). In the context of Alzheimer's disease (AD), HTRA1 has been shown to degrade both amyloid-beta and tau proteins, indicating a potential protective role against the formation of neurotoxic aggregates (Chen et al., 2024). Given its involvement in the clearance of these key proteins, HTRA1 has emerged as a critical regulator of AD pathology. Research on this protein is essential for understanding how its function influences protein aggregation, neuroinflammation, and disease progression.

Despite the growing interest in HTRA1's role in Alzheimer's disease (AD), significant gaps remain in our understanding of its precise molecular interactions and potential as a therapeutic target (Zurawa-Janicka et al., 2010). To address this, we employ a multistage computational approach to identify viable HTRA1 inhibitors, screen a library of compounds, and evaluate their druggability using molecular docking, dynamics simulations, and toxicity assessments. Our results offer promising insights into HTRA1's potential as a therapeutic target, with lead compounds exhibiting strong binding affinities and favorable pharmacokinetic properties. This research lays the groundwork for future in vitro and in vivo validation, aiming to modulate HTRA1 activity and slow or prevent the progression of Alzheimer's disease.

2. Methods
2.1 Binding Site Identification

Three independent computational tools – DogSiteScorer, FTSite, and PrankWeb – were utilized to identify potential binding sites within the target protein structure. Each method employs distinct algorithms to predict ligand-binding pockets and comprehensively analyzes their characteristics. DogSiteScorer uses the DOG (Depth-oriented Grid) algorithm, which divides the protein surface into a grid and evaluates binding affinities, shape complementarity, and solvent accessibility. FTSite applies the Fast Fourier Transform (FFT) algorithm to assess pocket volume, hydrophobicity, and surface curvature, identifying sites by comparing the geometric properties of the protein surface with those of potential ligands. PrankWeb utilizes the PRANK algorithm, which combines solvent-accessible surface area (SASA), protein flexibility, and electrostatic potential, while considering parameters such as hydrogen bond donors and acceptors, cavity size, and surface entropy to predict and assess the druggability of binding pockets. Together, these tools provide a comprehensive and complementary analysis of potential binding sites by evaluating structural and energetic parameters.

2.1.1 DogSiteScorer

DogSiteScorer, a structure-based binding site prediction tool, was used to assess the geometric and physicochemical properties of the target protein. The input consisted of the protein's three-dimensional structure, which was uploaded to the DogSiteScorer web server. The tool then segmented the protein into potential pockets based on size, depth, enclosure, and hydrophobicity. The resulting binding sites were ranked according to their druggability score.

2.1.2 FTSite

FTSite, a computational solvent mapping approach, was employed to identify energetically favorable binding sites. The protein structure was provided in PDB format, and the algorithm used probe molecules to detect interaction hotspots. FTSite then ranked these sites based on their binding affinity and physicochemical properties, thereby refining binding site predictions.

2.1.3 PrankWeb

PrankWeb, a machine-learning-based predictor, was applied to validate binding site locations further. The protein structure was analyzed using PrankWeb's deep learning model, which integrates structural features to predict binding pockets. The tool assigned confidence scores to each predicted site, allowing for comparative analysis with results from DogSiteScorer and FTSite.

2.2 Ligand Screening and Evaluation

2.2.1 Pharmacophore-Based Screening with Pharmit

Pharmit was employed to screen potential ligand candidates based on pharmacophore features. A pharmacophore model incorporating various donor and acceptor combinations was designed to filter compounds with optimal binding potential. The top 15 candidates were selected based on different combinations of donor and acceptor features, ensuring structural diversity and binding efficacy.

2.2.2 SwissDock Evaluation

The selected 15 ligand candidates were further analyzed using SwissDock, a molecular docking tool, to predict binding affinities and interaction modes. Each ligand's docking score and interaction profile were assessed to rank the top-performing molecules. Based on these evaluations, the top five ligands were se-

lected based on their lowest estimated binding free energies (ΔG values) and favorable full fitness scores, which reflect both binding affinity and ligand-protein interaction stability. Ligands exhibiting the most negative ΔG values and robust interaction profiles – characterized by consistent hydrogen bonding, hydrophobic contacts, and favorable binding poses within key active site residues – were prioritized for further molecular dynamics simulation and ADMET analysis.

2.3 ADME Analysis with SwissADME

The top five ligand candidates were analyzed using the SwissADME tool. This tool predicts key pharmacokinetic properties, including lipophilicity (LogP), solubility, GI absorption, BBB permeability, and drug-likeness, based on rules such as Lipinski's Rule of Five. This step helped identify compounds with favorable bioavailability and therapeutic potential.

2.4 Toxicity Prediction with ProTox-3

The best-performing ligand from the ADME analysis was further assessed for potential toxicity using ProTox-3.0. This tool provided insights into possible toxic effects, including hepatotoxicity, carcinogenicity, and overall safety profile, ensuring that the selected candidate was both effective and safe for further development.

3. Results

3.1. Identification of binding sites in HTRA1

3.1.1. Protein Surface Geometry and Binding Site Prediction Using DoGSiteScorer

P_0 and P_1 stand out as the most promising binding sites, with high volumes (663.81 and 628.74 Å³, respectively) and surface areas (841.34 and 861.36 Å²), coupled with the highest drug scores (0.79 and 0.86). These values suggest that these sites may provide favorable environments for ligand binding. The binding pockets were identified using **Protein Plus**, a geometric analysis tool that evaluates protein cavities based on volume, surface area, and druggability. Typically, volumes between 200––600 Å³ and drug scores above 0.5 are considered promising for small-molecule binding, and both P_0 and P_1 exceed these thresholds. In contrast, sites like P_10 and P_11

have significantly lower drug scores (0.37 and 0.23) and smaller volumes, making them less attractive for drug targeting. Interestingly, P_6, despite having an extremely low volume (2.53 Å³), exhibits a moderate drug score (0.56), possibly due to its high surface area (457.45 Å²), which suggests a unique binding feature. Overall, P_0 and P_1 are the most viable candidates for further drug design efforts targeting HTRA1.
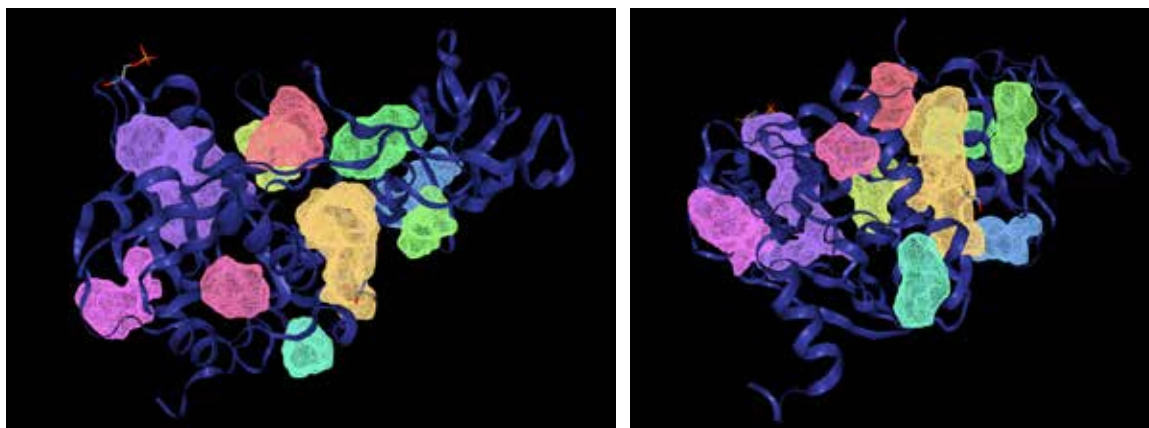
Figure 1. *Binding sites in HTRA1 displayed as colored spheres based on ProteinPlus.*

Table 1. *Data from top ten detected binding site in HTRA1 using ProteinPlus*

Name	Volume	Surface Area	Druggability Index
P_0	663.81	841.34	0.79
P_1	628.74	861.36	0.86
P_10	131.78	436.67	0.37
P_11	121.92	233.27	0.23
P_2	264.38	359.39	0.45
P_3	244.03	506.08	0.36
P_4	240.32	406.2	0.52
P_5	234.88	342.63	0.48
P_6	2.5314	457.45	0.56
P_7	203.33	286.55	0.39

Graph 1. *3D Scatter Plot of Molecular Properties: Volume, Surface Area, and Druggability Index*

HTRA1-TARGETED SMALL MOLECULES AS THERAPIES FOR ALZHEIMER'S DISEASE
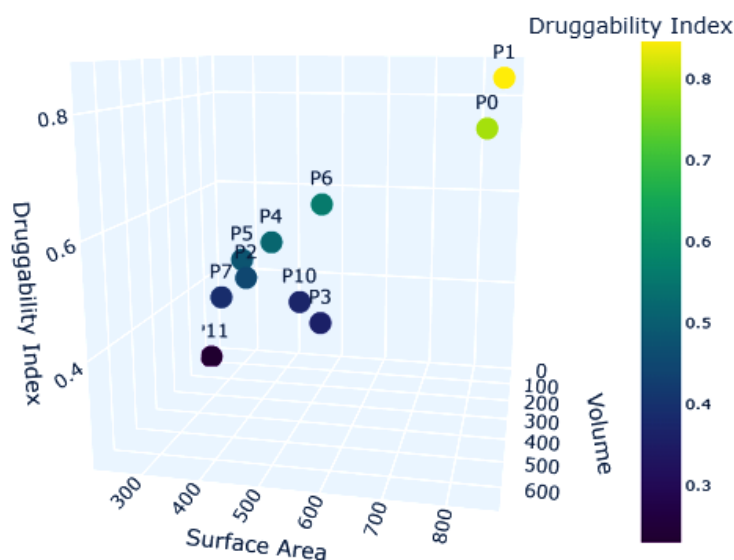
3.1.2. Energetic Profiling for Ligand Binding Site Identification with FTSite

Figure 2. *Binding sites in HTRA1 as predicted by the energetic method*
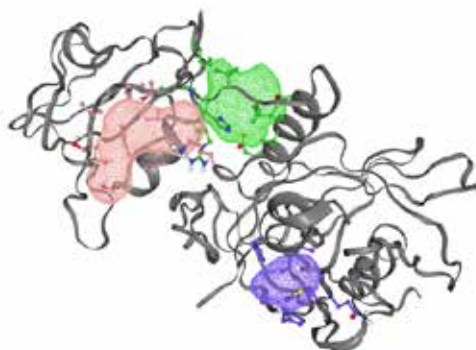
3.1.3.Machine learning methods

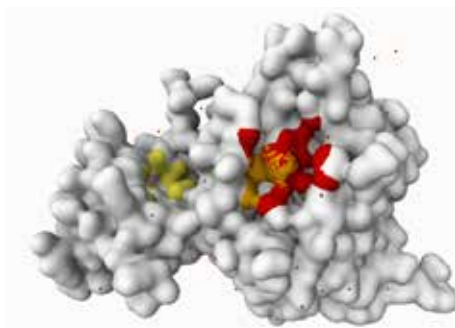**Figure 3.** *Binding sites in HTRA1 as predicted by Prankweb*

Table 2. *Analysis of the binding sites identified by Prankweb in the HTRA1 protein*

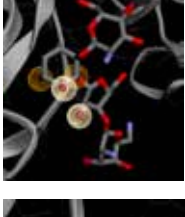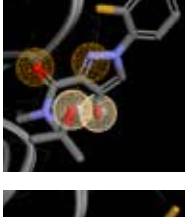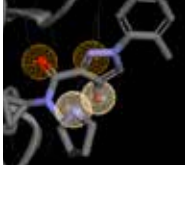| Rank	Score	Probability	#residues	Avg conservation
1.	5.05	0.240	10	1.827
2.	1.53	0.022	10	1.273
3.	1.49	0.021	6	1.975
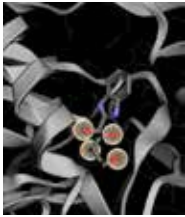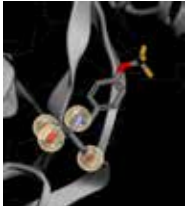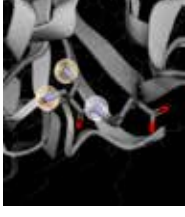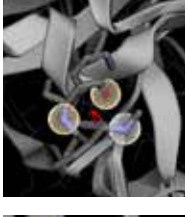
The highest-ranked pocket (Rank 1) has a score of 5.05 and a 24.0% probability, suggesting a moderate chance of being a viable drug target. This site also contains 10 residues with an average conservation score of 1.827, indicating a relatively conserved region that may be favorable for drug binding. In contrast, the second and third-ranked pockets have significantly lower probabilities (2.2% and 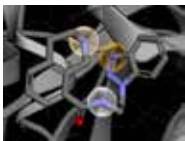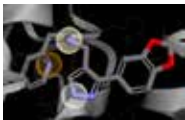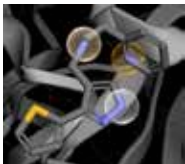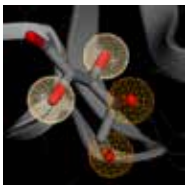2.1%), making them less attractive for drug development. The third pocket, despite its lower rank, has the highest average conservation (1.975), which could suggest functional importance. Overall, the first-ranked site appears to be the most promising target, but its moderate probability suggests that further validation, such as molecular docking studies, would be necessary to confirm its druggability.
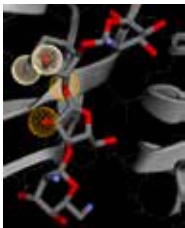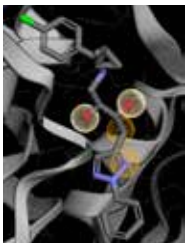
3.2. Pharmacophore-based screening

Table 3. *The outcome of the pharmacophore-based screening and top hit compounds*

	Name	RMSD	Mass	RBnds	Photo
4 donors and 4 acceptors	Z460996690	0.201	382	12	

	Name	RMSD	Mass	RBnds	Photo
	Z56762860	0.201	68	5	
	Z1946857219	0.203	295	8	
	Z4900394450	0.037	269	5	
3 Donors, 2 Acceptors	Z1731274937	0.042	290	6	
	Z1079047778	0.044	317	7	
	Z1551627167	0.115	616	9	
2 Donors, 4 Acceptors	Z1548358070	0.152	321	6	
	Z1762139434	0.170	358	6	

HTRA1-TARGETED SMALL MOLECULES AS THERAPIES FOR ALZHEIMER'S DISEASE

	Name	RMSD	Mass	RBnds	Photo
	Z3699434447	0.010	321	5	
2 Donors, 2 Acceptors	Z871870844	0.012	322	6	
	Z1162944959	0.012	284	6	
	Z1255372712	0.100	150	4	
2 Donors, 4 Acceptors	Z1551627167	0.121	616	9	
	Z1595791252	0.153	443	9	

Graph 2. *3D Plot of Chemical Properties: Mass, Rotatable Bonds, and RMSD*
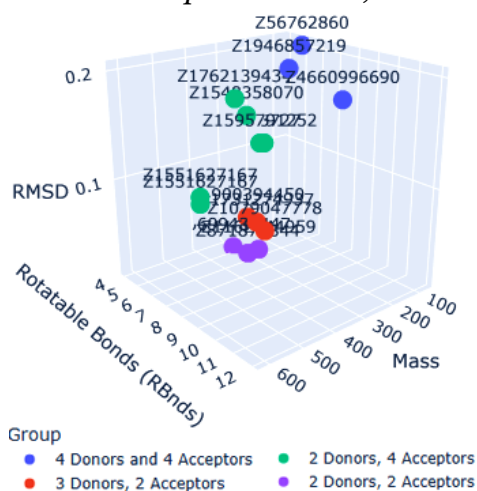
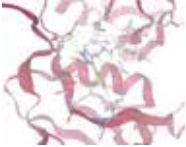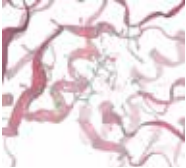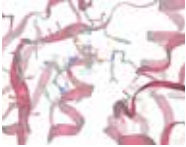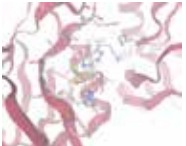The pharmacophore screening identified several potential HTRA1-binding molecules, categorized based on the number of hydrogen bond donors and acceptors, RMSD values, molecular weight, and flexibility (as indicated by the presence of rotatable bonds).
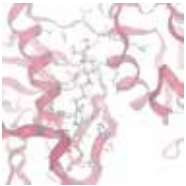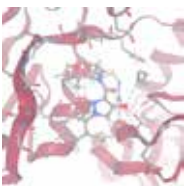
Lower RMSD values indicate better structural alignment, making them a key factor in candidate selection. Among the tested compounds, those with two donors and two acceptors (e.g., Z3699434447, RMSD = 0.010) and three donors and two acceptors (e.g., Z4900394450, RMSD = 0.037) demonstrated the lowest RMSD, suggesting a strong pharmacophore fit despite fewer hydrogen bonding interactions. In contrast, molecules in the 4 donors, 4 acceptors category, such as Z1946857219 (RMSD = 0.203), exhibited higher RMSD values, indicating weaker alignment but potentially stronger binding affinity due to the presence of more hydrogen bonding sites. Compounds in the two donors, four acceptors group (e.g., Z1551627167, RMSD = 0.115) exhibited moderate RMSD values, with Z1551627167 appearing twice, suggesting structural adaptability. While low RMSD compounds may offer the best pharmacophore match, molecular weight and flexibility must also be considered, as overly rigid or large molecules could impact bioavailability. Further molecular docking and ADMET studies are necessary to refine these hits into viable drug candidates.

3.3. Docking experiment to evaluate HTRA1 binding affinity

Table 4. *Cluster Analysis of Compounds with AC Score and SwissParam Values*

Name	Cluster #	Cluster member	AC Score	Swiss Param	Photo
Z1162944959	5	1	0.405393	−7.0160	
Z871870844	0	1	−2.819263	−7.2444	
Z56762860	0	1	50.795203	−6.6629	
Z1946857219	1	1	35.487063	−6.9241	
Z4900394450	6	1	−80.246998	−7.0185	
Z1079047778	1	1	6.383523	−6.9815	

Name	Cluster #	Cluster member	AC Score	Swiss Param	Photo
Z4660996690	1	1	−26.996090	−7.8131	
Z1255372712	1	1	29.370701	−6.0617	
Z1548358070	0	1	21.860387	−7.5094	
Z1762139434	0	1	242.297407	−8.0047	
Z3699434447	9	1	0.837294	−7.2267	
Z1551627167	4	1	249.209687	−8.2061	
Z1548358070	9	1	13.396534	−6.9062	
Z1731274937	0	1	−56.103916	−6.7996	

Graph 3. *3D Cluster Analysis of Compounds: AC Score,
SwissParam, and Cluster Assignment*
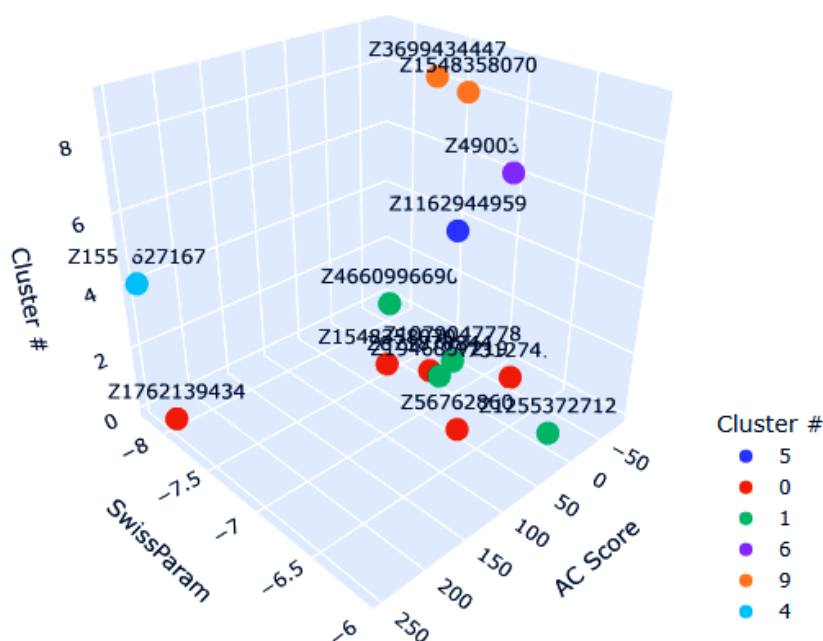
Molecular docking is a computational technique used to predict the preferred binding orientation of molecules to a target receptor, thereby helping to determine potential drug candidates. This study performed docking simulations for multiple candidate molecules using SwissDock, analyzing their cluster numbers, AC Scores, and SwissParam Scores to assess binding affinity and stability. Among the candidates, Z1162944959 exhibited moderate binding affinity with an AC Score of 0.405393 and a SwissParam Score of −7.0160, suggesting a stable but not the strongest binding. Z871870844 demonstrated a stronger interaction with an AC Score of −2.819263 and a SwissParam Score of −7.2444, indicating better stability. Z56762860, with an AC Score of 50.795203 and a SwissParam Score of −6.6629, showed weak binding affinity. Z1946857219 had a slightly better interaction with an AC Score of 35.487063 and a SwissParam Score of −6.9241. The strongest binding candidate appeared to be Z4900394450, which had an AC Score of −80.246998 and a SwissParam Score of −7.0185, suggesting exceptional affinity and stability. Z1079047778 had a moderate AC Score of 6.383523 and a SwissParam Score of −6.9815. Z4660996690 exhibited strong binding with an AC Score of −26.996090 and a highly negative SwissParam Score of −7.8131. Z1255372712 had an AC Score of 29.370701 and a weaker SwissParam Score of −6.0617. Z1548358070 showed mixed results, with AC Scores of 21.860387 and 13.396534 and SwissParam Scores of −7.5094 and −6.9062, respectively. Z1762139434 displayed an extremely high AC Score of 242.297407 but a powerful binding potential with a SwissParam Score of −8.0047. Z3699434447 exhibited moderate interaction, with an AC Score of 0.837294 and a SwissParam Score of −7.2267. The strongest binder overall was Z1551627167, with an AC Score of 249.209687 and a SwissParam Score of −8.2061, indicating a highly stable interaction. Z1731274937 exhibited a significant binding potential, as noted in an AC Score of −56.103916 and a SwissParam Score of −6.7996. In conclusion, the best candidates for further investigation based on binding affinity and stability are Z4900394450, Z4660996690, and Z1551627167, which exhibited the most negative AC and SwissParam Scores, suggesting strong receptor interactions. Future studies should focus on validating these findings experimentally to confirm their potential as drug candidates.

3.4. Evaluation of the ADME properties for the top compounds using SwissADME

Table 5. *Physicochemical Properties of Top Five Candidates*

Property	Z1551627167	Z1762139434	Z4660996690	Z1548358070	Z871870844
Formula	C23H-47N5O18S	C19H24ClF-N4O2	C18H27F-N4O4	C16H20F-N3O3	C18H19Cl-N4O2
Molecular weight (g/mol)	713.71	394.87	382.43	321.35	358.82
Heavy atoms (count)	47	27	27	23	25
Aromatic heavy atoms (count)	0	11	10	11	17
Fraction Csp3	1.00	0.47	0.56	0.38	0.22
Rotatable bonds (count)	9	6	12	6	6
H-bond acceptors (count)	23	5	8	5	5
H-bond donors (count)	15	2	5	2	2
Molar refractivity	147.78	106.70	99.61	83.87	96.72
TPSA (Å²)	430.30	70.39	119.64	78.59	72.06

Table 6. *Lipophilicity Metrics of Top Five Candidates*

Lipophilicity Metric	Z1551627167	Z1762139434	Z4660996690	Z1548358070	Z871870844
iLOGP	−0.32	0.00	2.61	2.30	0.00
XLOGP3	−12.39	3.83	−1.32	2.28	2.78
WLOGP	−8.43	3.16	−0.37	2.37	3.18
MLOGP	−8.28	2.46	−0.26	1.53	1.42
SILICOS-IT	−8.90	2.22	1.59	1.47	3.68
Consensus Log P	−7.66	2.33	0.45	1.99	2.21

The top candidate is Z1551627167, primarily due to its high polarity, as indicated by its large TPSA of 430.30 Å² and a consensus Log Po/w of −7.66. With a molecular weight of 713.71 g/mol, this compound is highly hydrophilic and likely to interact strongly with polar biological systems, making it suitable for applications in aqueous environments where strong hydrogen bonding is crucial. However, its low lipophilicity suggests that it would have a limited ability to cross biological membranes, restricting its use to environments such as blood plasma or extracellular fluids. Following Z1551627167, Z1762139434 stands out with a smaller molecular weight of 394.87 g/mol and a more balanced lipophilic profile (Log Po/w of 2.33), which suggests it can more easily penetrate cell membranes and could be used for intracellular targeting. Other candidates, such as Z4660996690, Z1548358070, and Z871870844, fall between the two, offering moderate lipophilicity and varying levels of polarity, making them more versatile but less specialized. Ultimately, Z1551627167 and Z1762139434 remain the top contenders, with Z1551627167 excelling in polar interactions and Z1762139434 offering greater flexibility in membrane permeability.

3.5. Evaluation of the toxicity of the top compound Z1551627167

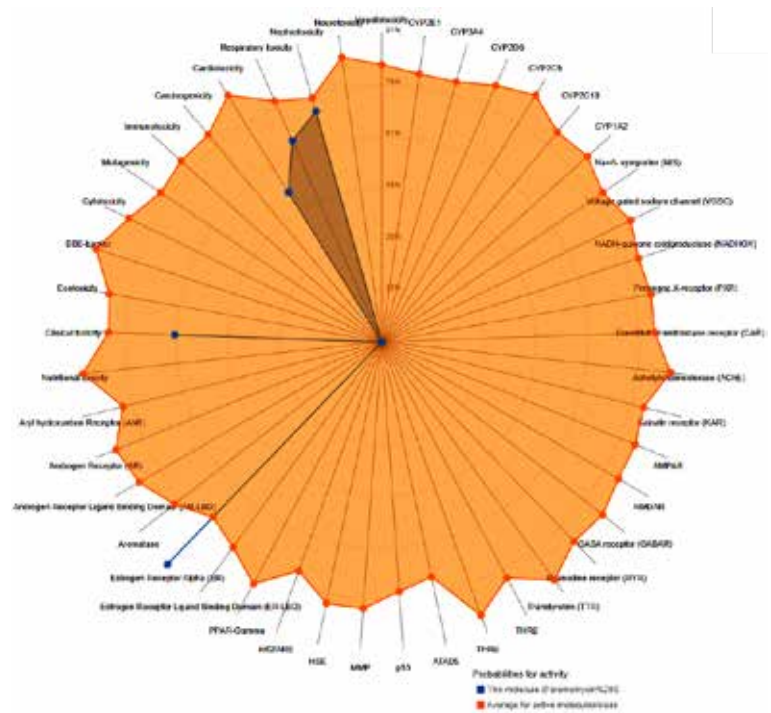**Figure 4.** *Toxicological and Physicochemical Profile*

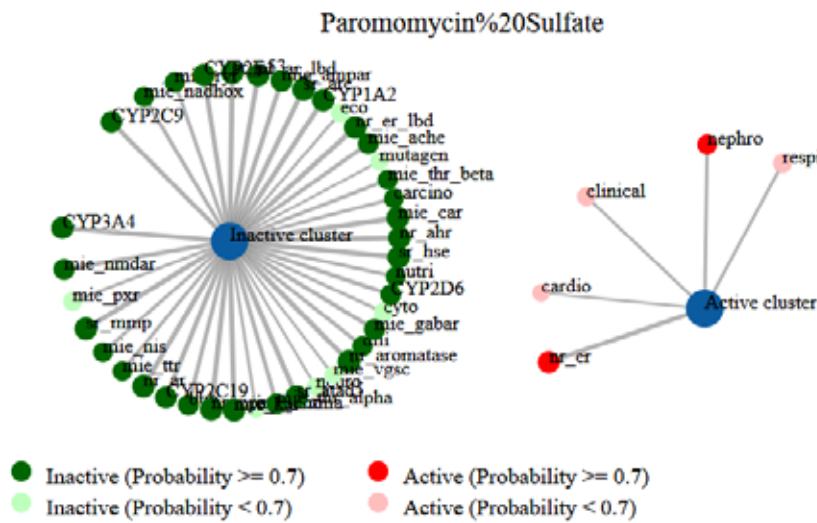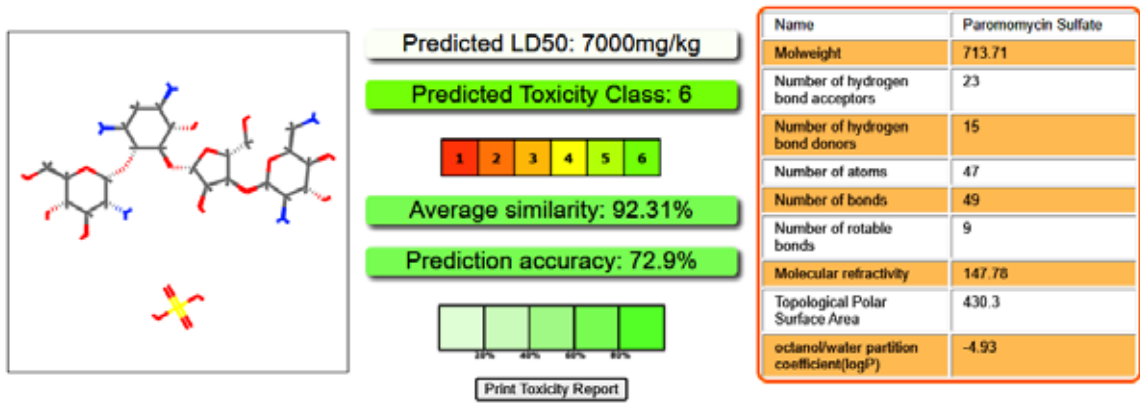**Figure 5.** *Radar Plot of Predicted Biological Activities and Toxicological Endpoints*

Figure 6. *Toxicity report*

HTRA1-TARGETED SMALL MOLECULES AS THERAPIES FOR ALZHEIMER'S DISEASE

The toxicity report for Z1551627167 (Paromomycin Sulfate) indicates a predicted LD50 of 7000 mg/kg, placing it in Toxicity Class 6, which suggests that it is moderately toxic. The Toxicity Class 6 classification is typically reserved for substances that may pose a health risk with repeated or prolonged exposure. Still, their lethal dose is relatively higher compared to compounds in higher toxicity classes. The report also highlights that the average similarity of 92.31% and prediction accuracy of 72.9% provide a solid basis for this toxicity classification. However, it's essential to note that toxicity predictions are often based on in silico models, and actual toxicity may vary under different biological conditions.

The compound's molecular weight of 713.71 g/mol and a topological polar surface area (TPSA) of 430.3 Å² suggest it is highly polar, which might limit its ability to cross cellular membranes easily. The number of hydrogen bond acceptors (23) and hydrogen bond donors (15) indicates a significant potential for interactions with biological targets, possibly influencing its toxicity profile by affecting cellular processes. The octanol/water partition coefficient (logP) of −4.93 confirms its high hydrophilicity, which may limit membrane permeability but could enhance its solubility in aqueous environments, making it more bioavailable in fluids such as plasma.

4. Discussion

In this study, a multi-tiered computational strategy was employed to identify and evaluate potential drug-binding sites on HTRA1, aiming to discover promising small-molecule inhibitors. Initial binding site analysis using ProteinPlus revealed that binding pockets P_0 and P_1 are the most viable candidates for drug targeting. These sites demonstrated large cavity volumes (663.81 and 628.74 Å³) and surface areas (841.34 and 861.36 Å²), alongside drug scores of 0.79 and 0.86, significantly exceeding conventional thresholds for druggability. While other pockets like P_10 and P_11 exhibited far lower scores and volumes, making them less favorable, the atypical case of P_6, with its very low volume but moderate drug score, suggests that unique surface features may still contribute to niche binding potential. These findings strongly support prioritizing P_0 and P_1 in downstream drug design efforts.

Machine learning-based binding pocket prediction provided complementary insights, identifying a top-ranked site with a 24.0% probability of druggability. This site also contained a relatively conserved set of 10 residues (average conservation score: 1.827), suggesting potential functional significance. Although the second and third-ranked sites had markedly lower probabilities (2.2% and 2.1%), the third site's highest conservation score (1.975) raises the possibility of an overlooked functional domain. Nonetheless, the convergence between geometric and machine learning analyses affirms the viability of the top-ranked site, tentatively corresponding to P_0 or P_1, for further exploration.

To refine ligand selection, pharmacophore-based screening was performed using structural alignment and hydrogen bonding profiles. Molecules with 2–3 donors and two acceptors, such as Z3699434447 and Z4900394450, achieved the lowest RMSD values (0.010 and 0.037), indicating a strong pharmacophore fit despite fewer hydrogen bonding groups. On the other hand, compounds with more donors and acceptors (e.g., Z1946857219) showed higher RMSDs, suggesting less favorable alignment, possibly due to conformational strain. Z1551627167 emerged as an up-and-coming candidate, appearing across multiple pharmacophore categories with moderate RMSD and notable structural adaptability, reinforcing its potential for further investigation.

Molecular docking simulations provided a more detailed assessment of ligand-receptor interactions. Among the compounds tested, Z4900394450 exhibited the strongest binding affinity (AC Score = −80.246998) and favorable SwissParam stability (−7.0185). Z4660996690 and Z1551627167 also demonstrated high-affinity interactions, with highly negative SwissParam Scores (−7.8131 and −8.2061, respectively), suggesting robust binding stability. The docking results further validated the pharmacophore predictions and highlighted Z1551627167 as a leading candidate, particularly given its recurring presence across multiple evaluation platforms. Other compounds, such as

Z1762139434 and Z871870844, also showed promise, albeit to a lesser degree.

To assess drug-likeness and pharmacokinetic properties, an ADME (Absorption, Distribution, Metabolism, and Excretion) profile was conducted using SwissADME. Z1551627167 stood out for its high polarity (TPSA = 430.30 Å²) and extreme hydrophilicity (Log Po/w = −7.66), indicating a strong potential for aqueous solubility but poor membrane permeability. This suggests its application may be best suited for extracellular targets, such as within blood plasma. In contrast, Z1762139434 presented a more drug-like profile, with a moderate molecular weight (394.87 g/mol) and balanced lipophilicity (Log Po/w = 2.33), allowing for better membrane diffusion and intracellular access. Other candidates exhibited intermediate characteristics, providing flexibility depending on the desired pharmacological target environment.

Toxicity analysis, based on in silico prediction models, classified Z1551627167 as Toxicity Class 6, with a predicted LD50 of 7,000 mg/kg, indicating moderate toxicity. While this relatively high LD50 implies a degree of safety under controlled exposure, the compound's high hydrogen bonding capacity (23 acceptors, 15 donors) and low logP (−4.93) suggest it may interact broadly with biological systems, potentially influencing its toxicity profile. These properties underline the importance of careful dosing and targeted delivery mechanisms to minimize off-target effects and improve therapeutic specificity. While Z1762139434 presented fewer toxicity concerns, further empirical testing is essential for both compounds to verify these predictions under physiological conditions.

In conclusion, this multimodal computational study identified P0 and P1 as the most promising druggable sites on HTRA1 and highlighted Z1551627167, Z4900394450, and Z1762139434 as top ligand candidates. Z1551627167 consistently demonstrated strong performance across pharmacophore alignment, docking, and ADME/Toxicity profiling, though its limited permeability and moderate toxicity warrant cautious consideration. Z1762139434, by contrast, offers a more balanced pharmacokinetic profile and may be more versatile for intracellular targeting. Future studies should prioritize experimental validation of these candidates through molecular dynamics simulations, in vitro binding assays, and in vivo pharmacological evaluations to fully assess their therapeutic potential.

References

Alzheimer's Association. (n.d.). *Medications for memory, cognition & dementia-related behaviors*. https://www.alz.org/alzheimers-dementia/treatments/medications-for-memory

Bartus, R. T., Dean, R. L., Beer, B., & Lippa, A. S. (1982). The cholinergic hypothesis of geriatric memory dysfunction. *Science, –* 217(4558). – P. 408–414. URL: https://doi.org/10.1126/science.7046051

Chen, S., Puri, A., Bell, B., Fritsche, J., Palacios, H. H., Balch, M., Sprunger, M. L., Howard, M. K., Ryan, J. J., Haines, J. N., Patti, G. J., Davis, A. A., & Jackrel, M. E. (2024). HTRA1 disaggregates α-synuclein amyloid fibrils and converts them into non-toxic and seeding incompetent species. *Nature Communications, –* 15(1). URL: https://doi.org/10.1038/s41467-024-46538-8

Cummings, J., Lee, G., Zhong, K., Fonseca, J., & Taghva, K. (2021). Alzheimer's disease drug development pipeline: 2021. *Alzheimer's & Dementia: Translational Research & Clinical Interventions, –* 7(1). – e12179. URL: https://doi.org/10.1002/trc2.12179

Hardy, J. A., & Higgins, G. A. (1992). Alzheimer's disease: The amyloid cascade hypothesis. *Science, –* 256(5054). – P. 184–185. URL: https://doi.org/10.1126/science.1566067

Hampel, H., Mesulam, M. M., Cuello, A. C., Farlow, M. R., Giacobini, E., Grossberg, G. T., Khachaturian, A. S., Vergallo, A., & Cummings, J. L. (2018). The cholinergic system in the pathophysiology and treatment of Alzheimer's disease. *Brain, –* 141(7). – P. 1917–1933. URL: https://doi.org/10.1093/brain/awy132

Heneka, M. T., Carson, M. J., El Khoury, J., Landreth, G. E., Brosseron, F., Feinstein, D. L., Jacobs, A. H., Wyss-Coray, T., Vitorica, J., Ransohoff, R. M., Herrup, K., Frautschy, S. A.,

HTRA1-TARGETED SMALL MOLECULES AS THERAPIES FOR ALZHEIMER'S DISEASE

Finsen, B., Brown, G. C., Verkhratsky, A., Yamanaka, K., Koistinaho, J., Latz, E., Halle, A., … Kummer, M. P. (2015). Neuroinflammation in Alzheimer's disease. *The Lancet Neurology,* – 14(4). – P. 388–405. URL: https://doi.org/10.1016/S1474-4422(15)70016-5

Heppner, F. L., Ransohoff, R. M., & Becher, B. (2015). Immune attack: The role of inflammation in Alzheimer disease. *Nature Reviews Neuroscience,* – 16(6). – P. 358–372. URL: https://doi.org/10.1038/nrn3880

Knopman, D. S., Jones, D. T., & Greicius, M. D. (2021). Failure to demonstrate efficacy of aducanumab: An analysis of the EMERGE and ENGAGE trials as reported by Biogen, December 2020. *Alzheimer's & Dementia,* – 17(4). – P. 696–701. URL: https://doi.org/10.1002/alz.12213

Kurkinen, M., Fułek, M., Fułek, K., Beszłej, J. A., Kurpas, D., & Leszek, J. (2023). The amyloid cascade hypothesis in Alzheimer's disease: Should we change our thinking? *Biomolecules,* – 13(3). – 453 p. URL: https://doi.org/10.3390/biom13030453

Lecca, D., Jung, Y., Scerba, M., Hwang, I., Kim, Y., Kim, S., Modrow, S., Tweedie, D., Hsueh, S., Liu, D., Luo, W., Glotfelty, E., Li, Y., Wang, J., Luo, Y., Hoffer, B., Kim, D., McDevitt, R., & Greig, N. (2022). Role of chronic neuroinflammation in neuroplasticity and cognitive function: A hypothesis. *Alzheimer's & Dementia,* – 18(11). – P. 2327–2340. URL: https://doi.org/10.1002/alz.12610

Orhan, I. E. (2021). Cholinesterase inhibitory potential of quercetin towards Alzheimer's disease – A promising natural molecule or fashion of the day? A narrowed review. *Current Neuropharmacology,* – 19(12). – P. 2205–2213. URL: https://doi.org/10.2174/1570159x18666201119153807

Scheltens, P., De Strooper, B., Kivipelto, M., Holstege, H., Chételat, G., Teunissen, C. E., Cummings, J., & van der Flier, W. M. (2021). Alzheimer's disease. *The Lancet,* – 397(10284). – P. 1577–1590. URL: https://doi.org/10.1016/S0140-6736(20)32205-4

Selkoe, D. J., & Hardy, J. (2016). The amyloid hypothesis of Alzheimer's disease at 25 years. *EMBO Molecular Medicine,* – 8(6). – P. 595–608. URL: https://doi.org/10.15252/emmm.201606210

Zurawa-Janicka, D., Skorko-Glonek, J., & Lipinska, B. (2010). HtrA proteins as targets in therapy of cancer and other diseases. *Expert Opinion on Therapeutic Targets,* – 14(7). – P. 665–679. URL: https://doi.org/10.1517/14728222.2010.487867

Contact: linwilliam0124@gmail.com